Award Accounts

The Chemical Society of Japan Award for Creative Work for 2002

Recent Developments in Studies of Electronic Excited States by Means of Electron Paramagnetic Resonance Spectroscopy

Seigo Yamauchi

Institute of Multidisciplinary Research for Advanced Materials, Tohoku University, Sendai 980-8577

Received January 16, 2004; E-mail: yamauchi@tagen.tohoku.ac.jp

New trends of electron paramagnetic resonance (EPR) are reviewed in studies of the electronic excited states conducted during this decade. The studies include EPR of excited triplet states in fluid solution and excited multiplet states in a triplet–radical pair system. Together with these new areas, advanced methods and techniques such as two dimensional pulsed EPR and high frequency high field EPR have been developed to analyze the new findings. In addition, time-resolved EPR with cw microwave has now become a general and very useful technique in time-domain experiments. Our recent works on porphyrins, phthalocyanines, and fullerenes are described in more detail.

EPR studies in the electronic excited states were focused until very recently mainly on the lowest excited triplet (T_1) state in solid.[1,2] More than 40 years passed after the first EPR signal had been observed for T_1 naphthalene in a single crystal of 1,2,4,5-tetramethylbenzene (durene) in 1958.[3] Two new streams have been reported in the mid-90's: one is studies on the T_1 state in fluid solution; the other is studies on excited multiplet states involving triplet–radical(s) pairs both in solid and fluid solutions. This article reviews these studies including several new results.

To observe the T_1 state in fluid solution was one of the big dreams for spin chemists, because almost all photochemical reactions occur in solution at room temperature and the T_1 states are very important precursors of the reactions in many cases. Till the 90's, the EPR data for T_1 in solid were used for analyses of the reactions in fluid solution. Although a technique of transient absorption provides very useful kinetic parameters for reaction intermediate species with high time resolution up to femto-seconds, poor information is obtained about their electronic structures. In contrast, EPR gives rise to detailed information for the electronic state and the electronic structure of the intermediates on the basis of zero-field splitting (ZFS) parameters and hyperfine coupling (hfc) constants. As for time resolution, the time-resolved EPR (TREPR) with cw microwave (MW) and Fourier transform pulsed MW EPR (FTEPR) techniques have resolution of 10–50 nano-seconds, which is usually good enough for the reaction from the T_1 state.

In 1992, the first TREPR spectrum was confirmed for the T_1 state in fluid solution on fullerene C_{60} at room temperature.[4] This observation was very exciting for spin chemists, but this turned out to be an exceptional case where the signal is extraordinarily sharp. The observed linewidth (0.045 mT) is much narrower than those of ordinary radicals. Such a too narrow signal does not include enough information on ZFS, which would provide detailed characteristics of the electronic state and structure in the T_1 states. In 1997, the T_1 spectra which involved moderate ZFS were observed for the first time in fluid solution by our group for porphyrins,[5] though the spectrum had been observed in mobile media such as liquid crystals by the Levanon group.[6] The spectra were observed in toluene solution from 5 to 360 K, where the spectral intensity does vary only by a factor of ca. 5–10 at around the melting point of toluene (178 K). We have extended the study to those of phthalocyanines and subphthalocyanine and analyzed these spectra in terms of dynamics of electronic structures and molecular motions. In this review, detailed paths from the findings to the analyses are described for the T_1 spectra in fluid solution.

For the excited multiplet state, although many people had tried to observe EPR signals in excited states other than a triplet, there was only one successful report on the triphenylene cation radical by Kothe et al.[7] Their idea for generation of excited multiplet states was to excite an ion ($S = 1/2$) having high symmetry and degenerate HOMO/LUMO states. These states, however, usually suffer from the Jahn–Teller distortion and provide a low spin state ($S = 1/2$) of very short lifetime. In that sense they were lucky to observe a quartet ($S = 3/2$) signal. Observations of the $\pi\pi^*$ and $d\pi^*$ excited states in metal complexes having a paramagnetic metal(s) center were also unsuccessful, due to the existence of low-lying dd states and/or short spin relaxation times.

A completely new and more general idea has appeared in two groups utilizing excited triplet state and stable nitoxide radical(s) pairs. In 1995, the Corvaja group reported a TREPR spectrum of the excited quartet (Q_1) state in a system of nitroxide-linked fullerene (C_{60}) in fluid toluene solution.[8] The Yamauchi group reported both on the Q_1 and doublet (D_1)
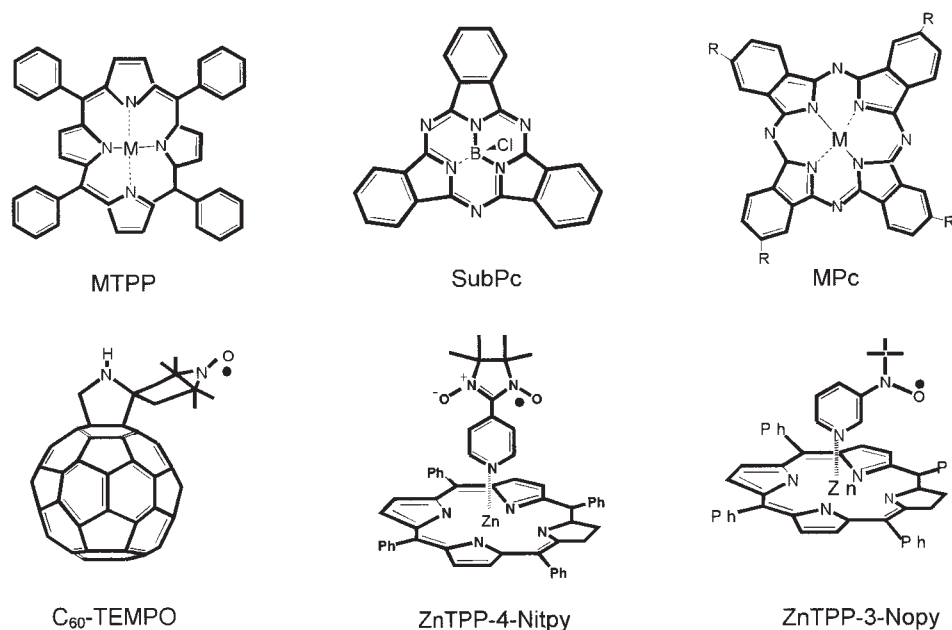
Fig. 1.   Molecular structures; MTPP: tetraphenylporphyrins (M = Zn, Mg, H_2), SubPc: boron subphthalocyanine, MPc: phthalo-cyanines (M = Zn, H_2), C_{60}-TEMPO, ZnTPP–4-Nitpy, and ZnTPP–3-Nopy.

states in solid toluene solution in a system of nitroxide ligated metal porphyrins.[9] The idea is based on the strategy that the excited triplet molecule couples with radical(s) strongly enough to generate new spin states and weakly enough to leave unchanged the characters of the triplet and the radical(s). Since then, the studies have been extended to various systems including different kinds of triplets and radicals and different numbers of radicals. Advanced EPR techniques such as two dimensional EPR and high field high frequency EPR have been developed to assign and separate the signals of different spin states. These studies are reviewed mainly focusing on our works.

The molecules used in this review are shown in Fig. 1.

Experimental Techniques

The TREPR technique was utilized at the X-band to observe transient EPR signals of the excited multiplet states including the T_1 state under cw MW irradiation both in fluid and solid solutions. The signals from a modified pre-amplifier of 10 MHz bandwidth in the microwave unit of the spectrometer (JEOL JES-FE-2XG) were integrated by an NF BX-531 boxcar to observe TREPR spectra at various delay times after the laser pulse and accumulated by an Iwatsu DM-7200 digital memory to obtain decay curves at finite magnetic fields. In these several years, the time profile of the signal is accumulated by the digital memory at every magnetic field and stored in a computer giving two dimensional (2D) EPR signals with respect to time and the field. From the 2D data, we can subtract both the TREPR spectra at finite times and the decay curves at arbitrary fields. A schematic diagram of the apparatus is shown in Fig. 2. One of the fundamental techniques used in cw EPR, magnetic field modulation, is not applied in TREPR to achieve higher time resolution. This procedure provides zero order MW emission (*E*) and/or enhanced absorption (*A*) signals instead of first derivative signals. The time resolution of our X-band system was ca. 100 ns and now is ca. 30 ns with an EF SA-230FS amplifier

of 100 MHz bandwidth. Temperature was controlled by an Oxford ESR 900 helium gas-flow system at 5–200 K and a JEOL ES-DVT3 cryo-system with nitrogen gas at 150–400 K. A Spectra Physics MOPO 730 OPO laser pumped by a Spectra Physics GCR 170 Nd:YAG laser was employed for excitation of molecule to the lowest spin allowed state in each case. The power of the OPO laser is 3–10 mJ/pulse at 10 Hz.

A time-resolved electron nuclear double resonance (TR-ENDOR) apparatus was constructed in our laboratory. The parts of microwave and the laser are the same as TREPR described above. A radio-frequency (RF) part includes those of the source (a SCITEC ADS-3-525), the amplifier (a KALMUS 166PL), and pulsing and timing circuits. This ENDOR equipment has been applied for the first time to the studies of the T_1 state of porphyrins in 1994.[10] For the quinoxaline triplet in a single crystal of durene, the ENDOR enhancement was achieved to 45% with respect to the intensity of the TREPR signal, and the signal could be observed up to 100 K.

At W-band (95 GHz), TREPR experiments were performed at room temperature using a laboratory-built EPR spectrometer in Berlin. The details of the apparatus are described in the literature.[11] We are now using a Bruker EMX W-band spectrometer with a modified light fiber and a broad band preamplifier for effective laser irradiation and high time resolution, respectively. The excitation of the molecules was done by using the 2nd harmonic 532 nm of a Nd:YAG laser or the Spectra Physics OPO laser. The time resolution of the system is ca. 20 ns, which is achieved by the NF SA-230F5 fast amplifier in our laboratory.

In 1997, we constructed an L-band EPR spectrometer with a loop-gap-resonator to observe the T_1 signal at nearly zero magnetic field in fluid solution. The spectrometer has abilities in sensitivity of 3×10^{11} spins/mT, time resolution of 80 ns, an MW power of 100 mW, and a cavity Q value of 600. Although we applied it to a study of porphyrins, we could not observe the T_1 signal in fluid solution but we did observe the ion pair spec-
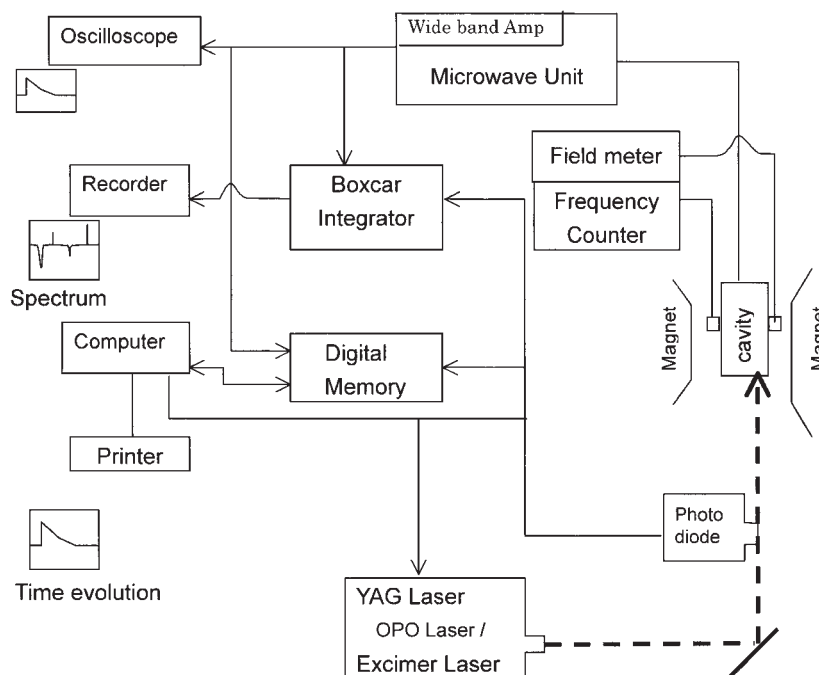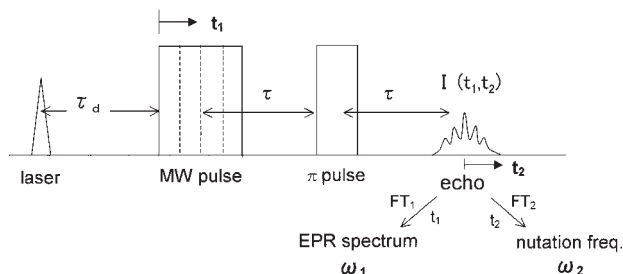
Fig. 2.　Time-resolved EPR apparatus.

Fig. 3.　Two dimensional pulsed nutation method.

Table 1.　Nutation Frequency ν_n and Spin State/Transition Assignment

S	Transition	ν_n/ν_1 [a]
1/2	$+1/2 \leftrightarrow -1/2$	1
1	$\pm 1 \leftrightarrow 0$	$\sqrt{2}$
3/2	$+1/2 \leftrightarrow -1/2$	2
	$\pm 3/2 \leftrightarrow \pm 1/2$	$\sqrt{3}$
2	$\pm 2 \leftrightarrow \pm 1$	2
	$\pm 1 \leftrightarrow 0$	$\sqrt{6}$

a) ν_1 is a nutation frequency of the doublet ($S = 1/2$) state.

trum in a photo-induced electron transfer system of porphyrin–quinone. Much higher sensitivity was needed for observation of the T_1 signal in solution.

A 2D pulsed nutation technique was developed using a laboratory-built pulse EPR machine in Sendai.[12] One pulse-free induction decay (FID) signals or two pulse-electron spin echo (ESE) signals were observed in liquid solution or solid solution by changing the first MW pulse width, as shown in Fig. 3. The typical parameters are shown for 2D in solid: the pulse width increases in 32 steps of 10 ns.[13] A nutated magnetization is focused by the second MW pulse of 110 ns width. The ESE signal was observed at each magnetic field and accumulated by an Evans Model 4130 gated integrator module with a sampling gate of 370 ns aperture. A nutation frequency (ν_n) is obtained by Fourier transformation (FT) of the ESE signals with respect to the first MW pulse width at each magnetic field (B_0), giving 2D spectra towards ν_n and B_0. From the nutation frequency, the spin state and the magnetic transition are assigned for the signals in the spectra on the basis of the following equation:[14]

$$\nu_n = [S(S+1) - M_S(M_S - 1)]^{1/2} \nu_1. \qquad (1)$$

Here ν_1 denotes the nutation frequency of a system of $S = 1/2$ under the condition examined. The nutation frequencies of sev-

eral spin systems are summarized in Table 1. More importantly, when the spectra are sliced at finite ν_n, a TREPR spectrum of a finite spin state is obtained for each transition.

The g value of the signal was calibrated with a very sharp line of triplet C_{60} ($g = 2.0012$) in toluene and/or six lines of a standard Mn^{2+}/MgO ($g = 2.00101$)[11b] crystalline sample. In the triplet-radical system, the g values of the nitronyl nitroxide pyridine (Nitpy) and N-oxy pyridine (Nopy) radicals (D_0) are used (2.0067 and 2.0059, respectively) to determine those of the Q_1 and D_1 signals.

Excited Triplet States in Fluid Solution

1. Fullerene. In 1991, two groups observed a surprisingly sharp TREPR signal having a half-width at the half maximum (HWHM) of 0.023 mT with an excitation of fullerene (C_{60}) in toluene fluid solution.[15] Although there were some doubts on its assignment in the beginning, it has been recognized as the T_1 signal.[4] This observation was very exciting for us spin chemists, because the observation of the T_1 spectra in solution was very important. The reason why we were waiting for the T_1 spectrum in solution is that fruitful information could be obtained on the T_1 structure from an analysis of the ZFS param-

eters. In that sense C_{60} is not sufficient. Although the analysis of ZFS has been made by Steren et al.,[16] the one sharp peak signal did not provide reliable information on the electronic structure. Actually, $^3C_{60}{}^*$ is an exceptional case of ultra high symmetry, where many Jahn–Teller split states are close together, and has the good fortune to give a very sharp signal due to fast averaging over signals of the states. Very weak spin polarization observed in fluid solution is consistent with this interpretation. For spin relaxations, spin–spin and spin–lattice relaxation times were measured for triplet C_{60} ($^3C_{60}{}^*$) by pulsed EPR and analyzed nicely in terms of the spin dipolar and spin rotation mechanisms. Anyway the observation of the $^3C_{60}{}^*$ signal has greatly stimulated us to challenge the T_1 signal in solution.

2. Metalloporphyrins. 2.1 First Observation: Here the process of finding the T_1 signal in solution is explained in more detail. Before 1995, nobody considered to be able to observe spectra of the T_1 states in fluid solution except for C_{60}. Even for C_{70}, no T_1 signal was observed in solution. To obtain some information on the T_1 state in solution, we examined the use of a technique of polarization transfer from the triplet to a radical (TRPT).[17] In this method, polarization generated in the triplet transfers to the stable radical and is observed via a polarized radical signal. We selected porphyrins as the triplet precursors. An advantage of these molecules is that polarization of the triplet is expected to vary with a change of central atom(s) (Zn, Mg, Cd, and H_2) in porphyrins on the basis of low temperature experiments. We used TEMPO as a typical radical. When porphyrins were excited by an OPO laser of 580–620 nm, spin polarized radicals were observed with moderate intensities; the polarity was different depending on the porphyrin, as shown in Figs. 4a–d. The observed net polarization is consistent with that
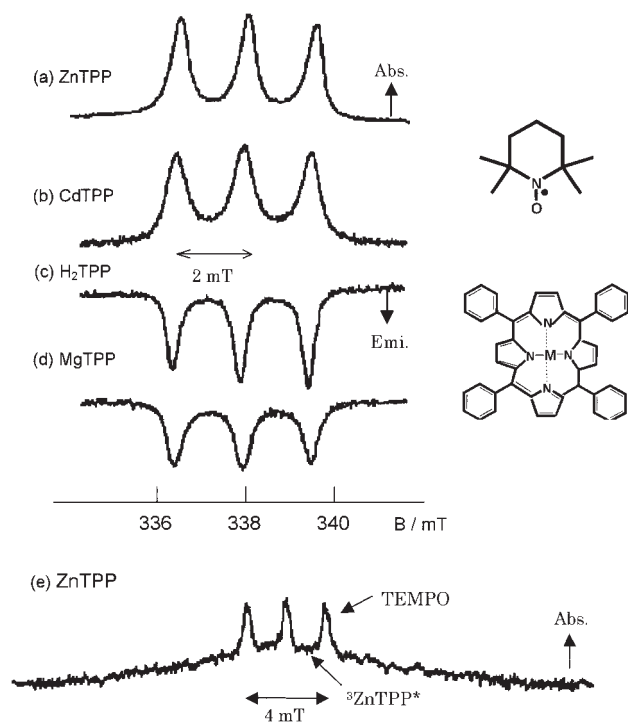
of T_1 porphyrin in solid and shows that the similar electronic T_1 state is involved also in fluid solution. In this experiment, we first used a magnetic field scan of ca. 5 mT for the three separated line signals due to the nitrogen (N) hfc of 1.9 mT (a_N). However, when we looked at the spectrum more carefully, we found a very slow rise and fall at much lower and higher field sides, respectively, on the TEMPO spectrum. Then we examined a wide range of scans over 50 mT and found a surprisingly broad one peak spectrum with HWHM of ca. 4.5 mT for the Zn tetraphenylporphyrin (ZnTPP)–TEMPO system, as shown in Fig. 4e. In all four porphyrins, such broad spectra were observed having the same polarization with the TEMPO radical, absorption (A) of microwave for ZnTPP and CdTPP and emission (E) for MgTPP and H_2TPP at earlier times. All the systems also provided a signal of a long life (tenths of µs) component having A polarization, which has the same decay rate as the transient optical absorption of the T_1 state. The decay of the fast component agreed well with a rise of generated polarization of the radical, which is consistent with polarization transfer from T_1 porphyrin to the radical. These facts confirmed that the observed broad spectra originated from the T_1 state in solution. This was an opening for the EPR studies on the T_1 state in fluid solution.

2.2 Observed Spectra and Decays in Solution: TREPR signals were obtained in a 2D manner as described in the experimental section for ZnTPP, Mg TPP, and H_2TPP in toluene at 10–360 K in a time range of −1 to 9 µs before and after the laser pulse. The decay curves showed fast and slow decaying components in all systems, where the slow component always shows an absorption of microwave. Typical decay curves are shown in Fig. 5. The fast decaying component reflects a CIDEP (chemically induced dynamic electron spin polarization) that comes from an anisotropy in an intersystem crossing (ISC) from S_1 to T_1 and decays with a spin–lattice relaxation process. The slow decaying component is due to a thermally averaged population of the spin state and decays with a lifetime of T_1. Thus the T_1 signal provides also kinetic information on T_1 in solution just like a transient absorption technique on a time scale of 30 ns. The TREPR spectra at 150 ns are shown in Figs. 6 and 7. The completely anisotropic spectra observed at low temperatures (<100 K) change spectral shapes and become gradually isotropic with increasing temperature. The sol-
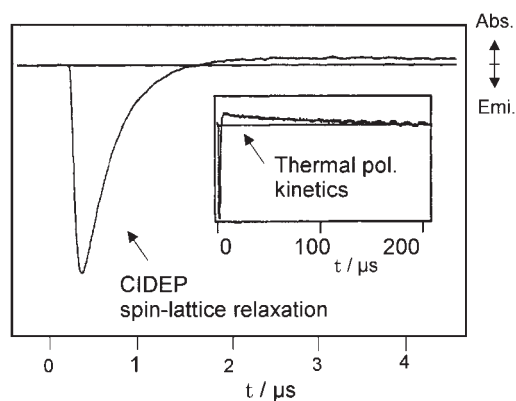

Fig. 4.   (a)–(d) Polarization transfer from excited triplet porphyrins to the TEMPO radical, and (e) observation of excited triplet ZnTPP (^{3}ZnTPP*).

Fig. 5.   Time-profile of the CIDEP signal for H_2TPP. The signal is composed of fast (emissive) and slow (absorptive) decay components.

S. Yamauchi

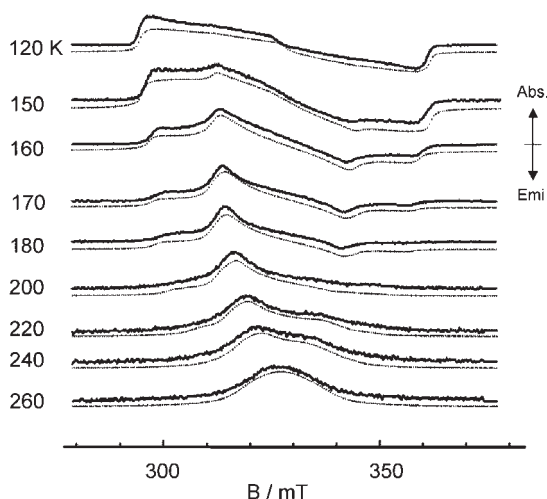*Bull. Chem. Soc. Jpn., 77, No. 7 (2004)* 1259

Fig. 6. Temperature dependence of the TREPR spectrum and their simulations for ZnTPP in toluene.
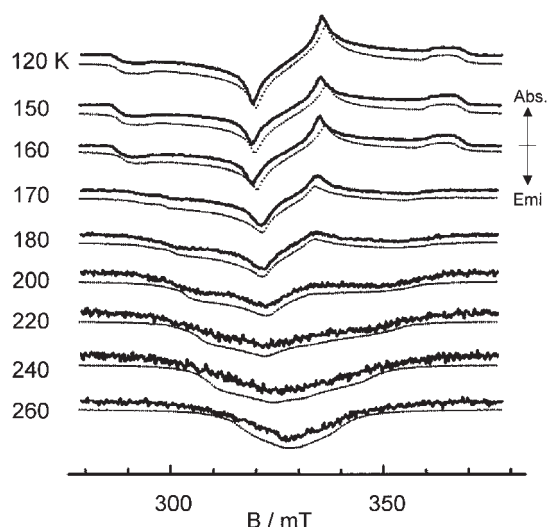

Fig. 7. Temperature dependence of the TREPR spectrum and their simulation for H_2TPP in toluene.

Table 2. Summary of Electronic Structures and Dynamics in MTPP at Various Temperatures

	ZnTPP	MgTPP	H_2TPP
10 K $\sim$	• Existence of the Jahn–Teller distortion (Symmetry reduction from D_{4h})		
		No temperature dependence	
100 K$\sim$	• Exchange between the Jahn–Teller split states ($\Delta E = 100\text{–}130$ cm^{-1})		
160 K$\sim$		Large effects due to the change in solvent phase	
170 K$\sim$	• Involvement of T_2 $\Delta E_{T1T2} = 240$ cm^{-1} (ZnTPP) 310 cm^{-1} (MgTPP)		• No T_2 involvement
	• Anisotropic to isotropic rotations ($\Delta E_\parallel = 400\text{–}500$ cm^{-1}, $\Delta E_\perp = 700$ cm^{-1})		• Isotropic but slow rotations ($\Delta E \sim 1350$ cm^{-1})
280 K$\sim$ $\sim$360 K		Isotropic rotation $\rightarrow$ Molecular radius a	
a	5.28 Å	5.26 Å	5.42 Å

vent melts at 178 K but the spectral intensity does change not so much, at most by a factor of 5, around the melting point. This is an important point in observing the T_1 spectra in fluid solution. Above 300 K, the spectra are isotropic showing a single Lorentzian line shape. We have analyzed these spectra on the basis of a four sites model that is described in the next section for subphthalocyanine.[18] As the complete analyses have not been published yet in the journals, only a part of the simulation and a summary of the analyses are also shown in Figs. 6 and 7 and Table 2.[19]

Here we consider the reasons why we could observe the spectra of the T_1 states in fluid solution. The suggestion by Weissman[20] that the signals are too broad to be observed in the T_1 state was partially correct. He calculated a linewidth $\Delta\omega_1$ of the EPR signal for the naphthalene triplet from a spin–lattice relaxation time T_{1d} with Eq. 2, which is obtained based on the spin dipolar mechanism for the two triplet spins in a medium size of molecules ($\omega^2 \tau_C^2 \gg 1$).[18]

$$\Delta\omega_1 = (1/2\pi)T_{1d}^{-1} \sim (2/15\pi)D^{*2}/(\omega^2 \tau_C), \quad (2)$$

$$\tau_C = 4\pi a^3 \eta / 3k_B T. \quad (3)$$

Here D^*, ω, τ_C, a, η, and k_B denote an effective ZFS value, an angular frequency, a rotational correlation time, the radius of the molecule, the viscosity of the solvent, and the Boltzmann constant. The typical line widths of 50–200 mT were obtained for fluid solution and are too large to be observed in the T_1 state. Our observations, however, showed that the linewidth $\Delta\omega_2$ was determined by a spin–spin relaxation time T_{2d} with Eq. 4, as demonstrated for phthalocyanine in the next section.

$$\Delta\omega_2 = (1/2\pi)T_{2d}^{-1} \sim (1/10\pi)D^{*2}\tau_C. \quad (4)$$

When we compare $\Delta\omega_1$ with $\Delta\omega_2$ (Eqs. 2 and 4), we find different τ_C dependence, which gives rise to reverse temperature and molecular size dependences (Eq. 3). It is also noted that T_{1d} is larger than T_{2d} by a factor of >10 even in fluid conditions ex-

amined. Another important factor beyond Weissman's consideration was strong spin polarization (CIDEP effect) involved in the TREPR experiment. In summary the conditions to observe the triplet spectra in fluid solution are the following; the molecules should have a smaller ZFS parameter D^* (Eq. 4) and a larger CIDEP effect. A larger size of molecule is preferable to observe the sufficient CIDEP effect with larger T_{1d} (Eq. 2) in the TREPR spectra. A group of porphyrins are such molecules with smaller $D^* = 38.2$ mT, larger $a = 5.3$ Å, and strong CIDEP.

3. Phthalocyanines. We tried to observe the TREPR spectrum of the T_1 state in fluid solution for other molecules and have immediately succeeded in observations of phthalocyanines (MPc: M = Zn, Mg, and H$_2$)[21] and subphthalocyanine (SubPc)[18] in toluene solution at 10–350 K. The analyses for SubPc are shown in the following.

3.1 Observed Spectra and Temperature Dependence: We selected boron(III) subphthalocyanine chloride (SubPc: Fig. 1) as a third triplet molecule in solution because of its smaller size and the unique structure of its C_{3v} symmetry.[18] The spectra observed at various temperatures for SubPc are similar to those of ZnTPP, as shown in Fig. 8. The observed polarization at 20 K is A, AAA/EEE, which means an absorption (*A*) of microwave at the $\Delta m = \pm 2$ transition, *A* at all three $\Delta m = \pm 1$ transitions of lower stationary fields ($B \parallel z$, y, and x), and an emission (*E*) at all three $\Delta m = \pm 1$ transitions of higher stationary fields, reflecting dominant anisotropic ISC to the lowest T_z sublevel in the T_1 state. The spectrum started changing anisotropically at 40 K, the lower temperature than that for ZnTPP and continued to change even at 360 K where the spectrum became isotropic. These spectra are simulated by the method described in the following.

3.2 Spectral Simulation: The temperature dependence of the triplet EPR spectra has been analyzed by two models; a rotational diffusion model[22] and a discrete jump model.[23] Our simulation is based on the advanced discrete jump model, by

which the jumps among N sites can be treated. The N sites have different ZFS, ISC ratios, and exchange rates k_{ex} among the sites. The sites can also include molecular rotations with the rate of k'_{ex}. These dynamics occur in an isotropic and/or an anisotropic (α, β, γ) manner, where the Euler angles, α, β, γ, reflect the anisotropy in the dynamics. The spin distribution of each site is described by the density matrices ρ_A, ρ_B, and so forth, which follow the Liouville equations:[18]

$$d\rho_A/dt = i[\rho_A, \hat{H}_A] + \sum_B (k_{BA}\rho_B - k_{AB}\rho_A) - \acute{R}_A(\rho_A - \rho_{A0}).$$

(5)

Here the Hamiltonian $\hat{H}_A$ is given by

$$\hat{H}_A = g\beta S \cdot B_0 + D_A\{S_z^2 - S(S+1)/3\} + E_A(S_x^2 - S_y^2).$$ (6)

k_{AB} is the exchange rate from A to B, $\acute{R}_A$ a generalized Redfield relaxation matrix, and ρ_{A0} the steady state density matrix. Following the Hudson and McLauchlan approach,[24] we write the solution of Eq. 4 for the EPR intensity versus ω in a given magnetic field $B (= \hbar\omega/g\beta)$ as

$$I(\omega) = 2ImTr\{\rho_0 S_x[1/(\Omega - \omega - i(\Pi + \acute{R}_A))]S_x\}.$$ (7)

The term S_x is the matrix representation for the Heisenberg spin operator of the triplet and Ω a $9N \times 9N$ supermatrix representing the commutator in Eq. 5 for the Hamiltonian of different sites. The supermatrices Π and $\acute{R}_A$ are related to the exchange and relaxation processes, respectively. Equation 7 is solved numerically for each molecular orientation at ω. Here we use an isotropic distribution function for a randomly oriented solution of toluene.

3.3 Analyses of the Spectra: The T_1 molecule was found to jump between two electronic states and to rotate anisotropically at low temperatures and isotropically at high temperatures. At 20 K, the spectrum was simulated with the ZFS parameters $D = 35.8$ mT and $|E| = 8.4$ mT and the ISC ratio of $P_z -$
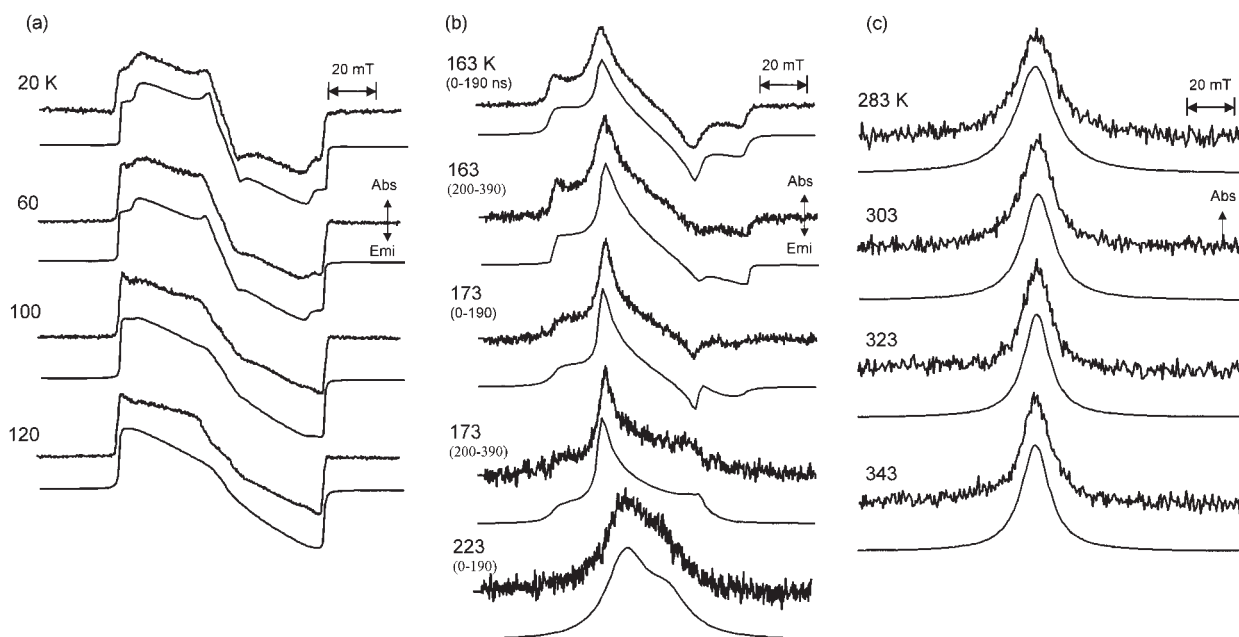

Fig. 8.   Temperature dependence of the TREPR spectrum and their simulations at a) 20–120 K, b) 163–223 K, and c) 283–343 K for SubPc in toluene.

S. Yamauchi

Bull. Chem. Soc. Jpn., **77**, No. 7 (2004)   1261

$P_x:P_y - P_x = 1:0$. The none-zero E value indicates that Jahn–Teller distortion occurs in the T_1 state. At 40–120 K, the spectrum starts to lose the clear peaks in the inner two canonical orientations ($B \parallel x, y$), while the outer-most peaks at the z orientation ($B \parallel z$) remain sharp. Here the z axis is perpendicular to the molecular plane. The spectra were simulated by the two sites (I and II) model described above, as shown in Fig. 8. The parameters used are $D_I = D_{II} = 35.8$ mT, $|E_I| = 8.4$ mT, $|E_{II}| = 11.9$ mT with slow exchange rates k_{ex}. The obtained rates were analyzed by the equation:

$$k_{ex} = k_{ex}{}^0 \exp(-\Delta E/kT) \tag{8}$$

and the values of $k_{ex}{}^0$ and ΔE were obtained as 6.5×10^7 s^{-1} and 57 cm^{-1}. From the DFT and PPP MO calculations, these two states (T_1 and T_2) were assigned to the Jahn–Teller split states in SubPc.

At intermediate temperatures of 163–243 K, the dynamics were analyzed by anisotropic exchanges and/or molecular motions. No other ZFS parameters are needed to simulate the spectra. The rates for in-plane and out-of-plane dynamics $k_\parallel$ and $k_\perp$ were obtained by Eqs. 9 and 10, respectively, where the values of α and β are temperature dependent, as summarized in Table 3:

$$k_\parallel = k_{ex}(\alpha/57°), \tag{9}$$

$$k_\perp = k_{ex}(\beta/57°). \tag{10}$$

From the Arrhenius plots of $k_\parallel$ and $k_\perp$ (Fig. 9) and the ratio of $k_\parallel/k_\perp$ (= α/β) (Table 3), we concluded that the dynamics in-

Table 3. Dynamic Parameters Obtained from the Spectral Simulation[a)] at 0–190 ns of SubPc

T/K	$k_{ex}/10^8$ s^{-1}	α/degree	β/degree	γ/degree
163	3.3	90	3	3
173	12 (2.9)[b)]	90	6	2
183	14 (5.6)	90	8	11
203	16 (17)	90	15	27
223	28 (39)	90	60	30
243	>28 (71)	90	75	40
263	>28	90	85	75

a) ZFS parameters: $D = 35.8$ mT and $|E| = 8.4$ mT. b) The values in parentheses are calculated $\tau_c{}^{-1}$ from Eq. 3 and $a = 4.5$ Å.
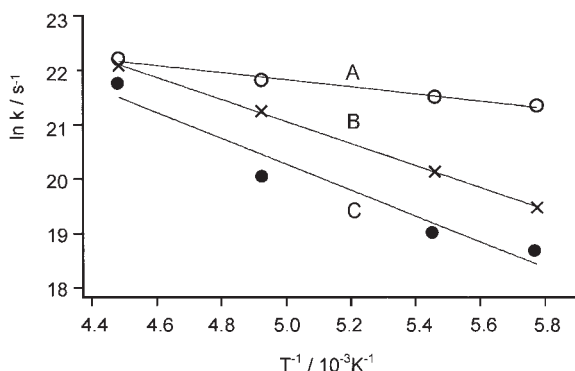

Fig. 9.   Arrhenius plots of exchange rate constants: A) $k_\parallel$, B) $\tau_r{}^{-1}$, and C) $k_\perp$.

Table 4. Observed Line Width $\Delta\omega$ and a Spin–Spin Relaxation Time T_2

T/K	$\Delta\omega$/MHz[a)]	T_2/ns[b)]	T_{2d}/ns[c)]
283	101	1.6	1.6
303	81	2.0	1.9
323	70	2.3	2.2
343	67	2.4	2.5

a) Half-width at the half maximum. b) $T_2 = 1/(2\pi\Delta\omega)$ (Eq. 11). c) Calculated from Eq. 12 with $a = 4.5$ Å.

volved are the in-plane and out-of-plane molecular rotations of SubPc with the activation energies of 420 and 1620 cm^{-1}, respectively.

At higher temperatures above 283 K, the spectrum becomes more isotropic and can be analyzed by a single Lorentzian line shape. From HWHM ($\Delta\omega$), a spin–spin relaxation time T_2 is obtained with Eq. 11 as summarized in Table 4.

$$T_2 = 1/(2\pi\Delta\omega). \tag{11}$$

These values are nicely realized with T_{2d} calculated by Eq. 12 with a molecular radius a of 4.5 Å (Eq. 3) on the basis of the spin dipolar relaxation mechanism.

$$T_{2d}{}^{-1} = (1/15)D^{*2}\tau_C[3 + 5/(1 + \omega^2\tau_C{}^2) + 2/(1 + 4\omega^2\tau_C{}^2)]. \tag{12}$$

Excited Multiplet States

Since the EPR signal of the T_1 state was first observed in 1958, an object of the EPR study in the excited state has been the triplet ($S = 1$) state. In 1980, Kothe et al. observed a TREPR signal in an excited quartet state ($S = 3/2$) for the mono-anion radical of decacyclene (DC$^-$)[7] whose di-anion (DC^{2-}) forms a famous triplet state due to its high symmetry in the ground state. Although this system was a very clever one to observe an excited multiplet state, no such states have been observed since then, probably because of the Jahn–Teller distortion occurring in the excited states. The Corvaja group[8] and our group[9] have tried independently to generate a completely new type of excited multiplet states using an excited triplet–radical(s) pair. The point of this system is that only a weak exchange interaction J ($J > D \sim 0.1$ cm^{-1}) between T_1 and radical(s) is needed to produce these excited multiplet states and no other limitations are involved. Here J is defined by $3J = E(D_1) - E(Q_1)$, where $E(D_1)$ and $E(Q_1)$ are electronic energies of the D_1 and Q_1 states, respectively. We started with the porphyrin system[25] and the Corvaja group started with the fullerene system[8] and both groups have succeeded in the observation of the excited quartet state.

The excited quartet ($S = 3/2$) and doublet ($S = 1/2$) states are generated in the T_1–mono-radical ($S = 1/2$) system. When two radicals ($S = 1/2 \times 2$) are involved in the system, the excited quintet ($S = 2$), triplet ($S = 1$), and singlet ($S = 0$) states are generated via the interactions of the triplet and radicals. The order of the state in energy is determined by the sign of J and depends on each system. In this study together with observations of new types of the excited states, advanced EPR techniques and methods were developed, and new polarization mechanisms were found. These are summarized in the following.
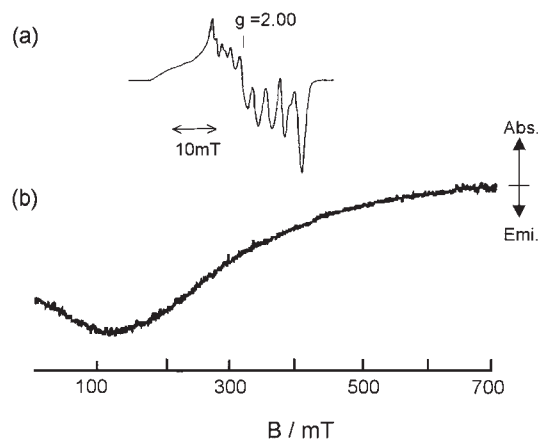
Fig. 10. a) Cw EPR spectrum and b) time-resolved EPR spectrum at 100 ns for O_2 ligated Co(II) tetraphenylporphyrin at 3.6 K in toluene.

1. Porphyrins and Phthalocyanines. 1.1 Solid State: We started with molecular oxygen ligated Co porphyrin [(dioxygen (tetraphenyl porphyrinato)cobalt(II); CoTPP] in which an unpaired electron on Co(II) interacts with one of the two unpaired electrons of O_2, leaving an unpaired electron ($S = 1/2$) on O_2 in the ground state. Complex formation and the spin structure are easily recognized from a cw EPR spectrum with small hfcc and g anisotropy (Fig. 10a). The spectrum spreads over ca. 38 mT centered at $g \sim 2.00$. When this complex was excited at 532 nm, a very broad and widely spread (0–700 mT) TREPR spectrum was observed at 3.6 K as shown in Fig. 10b.[9] This signal has net E polarization showing a weak temperature dependence and decays with 3 and 900 μs. This spectrum also differs remarkably from the Co(II)TPP complex whose spectrum spreads over ca. 260 mT. We tentatively assigned this broad signal as an excited quartet state ($S = 3/2$) that is composed of excited triplet porphyrin (^{3}TPP*; $S = 1$) and doublet oxygen ($S = 1/2$) and has a larger ZFS due to a large spin–orbit coupling effect of the central Co atom.[25]

Next we examined radical ligated metallo-porphyrins and got more reliable results on the excited multiplet states using (tetraphenylporphyrinato)zinc(II) (ZnTPP) ligated by a 4-pyridyl nitronyl nitroxide (Nitpy) radical in rigid toluene solution.[9] Observed TREPR spectra are compared at 20 K with that of pyridine ligated ZnTPP (ZnTPP–py) as shown in Fig. 11. The spectra of the radical ligated system (Figs. 11b and 11c) are very different from that in the T_1 state of ZnTPP (Fig. 11a) showing apparently a smaller ZFS. The net A spectrum observed at 25 μs (Fig. 11c) was simulated with the quartet state (Q_1) having ZFS parameters of $D = 0.25$ and $E = 0.08$ GHz under the Boltzmann (thermal) population. This is consistent with the fact that this A signal has the same decay time of 4.3 ms as that of the optical emission signal, which is much shorter than triplet ZnTPP–py (25 ms). The D value is in good agreement with the estimation (0.233 GHz) for $D(Q_1)$ from Eq. 13 with $D(T_1) = 0.912$ GHz and $D(RT_1) = -0.213$ GHz.

$$D(Q_1) = (1/3)[D(T_1) + D(RT_1)]. \tag{13}$$

The g value (2.004 ± 0.001) of the Q_1 state obtained from the center of the net A spectrum (Fig. 11c) was also consistent with Eq. 14[26] and with the values of $g(T_1)$ (= 2.0017) and $g(R)$
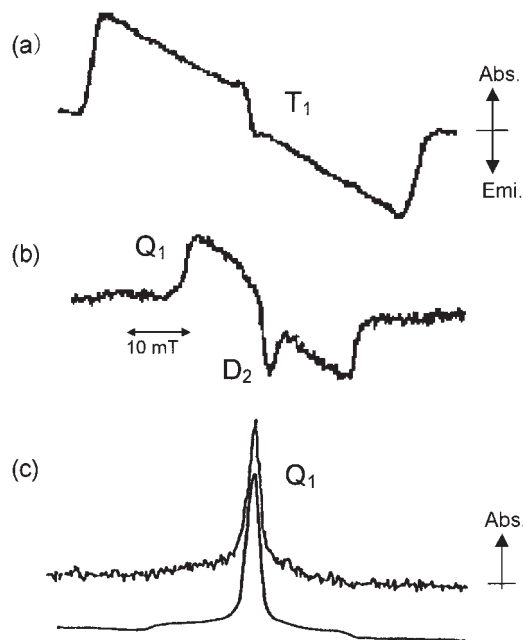

Fig. 11. Time-resolved EPR spectra of a) ZnTPP–py at 0.2 μs and of ZnTPP–4-Nitpy at b) 0.2 and c) 25 μs (with simulation) after the laser pulse and 20 K in toluene.

(= 2.0067). The net emissive peak at the central part ($g = 1.999 \pm 0.002$) of the spectrum (Fig. 11b) was assigned to an excited double (D_1) signal based on Eq. 15,[23] $g(T_1)$, and $g(R)$.

$$g(Q_1) = (1/3)g(R) + (2/3)g(T_1), \tag{14}$$

$$g(D_1) = (-1/3)g(R) + (4/3)g(T_1). \tag{15}$$

Later on, the spin polarized spectrum of the Q_1 (Fig. 11b) state was simulated using the spin Hamiltonian (Eq. 16), zero order wavefunctions (Eqs. 17a–d) of the Q_1 states, and the ISC ratio of $P_{\pm3/2}:P_{\pm1/2} = 1:0$.[27]

$$\boldsymbol{H}_{Q1} = \mu_B \boldsymbol{B} \cdot g_{Q1} \cdot \boldsymbol{S} + \boldsymbol{S} \cdot \boldsymbol{D}_{Q1} \cdot \boldsymbol{S}, \tag{16}$$

$$|Q_1, +3/2\rangle = |T_1, +1\rangle|D_0, +1/2\rangle, \tag{17a}$$

$$|Q_1, +1/2\rangle = \sqrt{1/3}|T_1, +1\rangle|D_0, -1/2\rangle$$
$$- \sqrt{2/3}|T_1, 0\rangle|D_0, +1/2\rangle, \tag{17b}$$

$$|Q_1, -1/2\rangle = \sqrt{1/3}|T_1, -1\rangle|D_0, +1/2\rangle$$
$$- \sqrt{2/3}|T_1, 0\rangle|D_0, -1/2\rangle, \tag{17c}$$

$$|Q_1, -3/2\rangle = |T_1, -1\rangle|D_0, -1/2\rangle. \tag{17d}$$

The TREPR spectra of the excited quartet and doublet states were observed in other porphyrin–radical systems, as shown in Fig. 12. The sign of J was evaluated from polarization of the D_1 signal to be positive for emissive signals and negative for absorptive ones, based on the radical–triplet pair type mechanism (RTPM type).[1b]

Ishii et al. have extended the studies to the radical–porphyrin (P) and/or –phthalocyanine (Pc) systems.[28] For the ZnPc–TEMPO and MgPc–TEMPO systems, opposite polarization was observed in the Q_1 spectrum and was interpreted in terms of selectivity in ISC that originated from T_1 ZnPc and MgPc. A
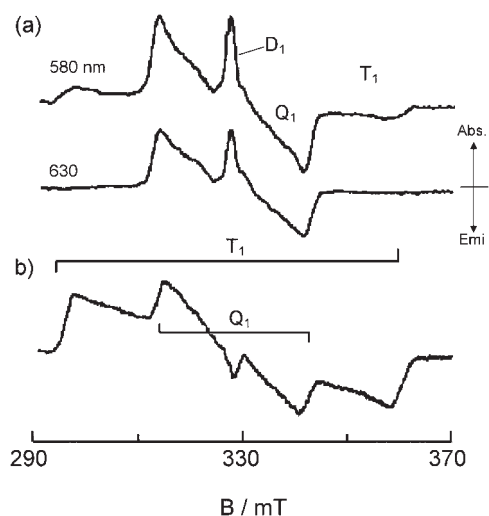
Fig. 12. Time-resolved EPR spectra of a) ZnTPP–3-Nopy and b) ZnTPP–4-Nopy at 20 K in toluene.

change from the T_1 to Q_1 spectrum was examined by changing the magnitude of the interaction (distance) between ZnTPP and a nitroxide radical (NRX; X = 4, 5, 8, 10 and denotes the bond number from Zn to the NO nitrogen). Around X = 8, the spectral change was observed.

1.2 X-Band and W-Band EPR in Fluid Solution: Surprisingly, signals of the excited multiplet states were also observed in fluid solution. At the X band, relatively strong signals were found in all systems examined in nitroxide radical-ligated MTPP (M = Zn and Mg) systems. Two examples are shown in Fig. 13, where the spectra were analyzed by those of the Q_1 and D_0 states as typically shown in Fig. 4 of Ref. 29. Polarization of the signal is interpreted in terms of interactions between the Q_1 and D_1 states and is dependent on the sign of J in the system. This is schematically illustrated in Fig. 14. When $J < 0$, absorptive polarization (A) is induced at the beginning for all the Q_1, D_1, and D_0 states via the RTPM type interaction. At later times, populations of the lower levels in both excited states become lower due to their faster decays providing reverse polarization of emission (E). So polarization inversion from A to E ($A \rightarrow E$) and E to A ($E \rightarrow A$) is expected to occur for the systems of $J < 0$ and $J > 0$, respectively. The D_0 signal is easily assigned from the steady state cw spectrum and the D_1 and Q_1 signals are assigned from the g value (Eqs. 14 and 15) and a hyperfine coupling constant (hfcc: a) (Eqs. 18 and 19).

$$a(Q_1) = (1/3)a(R) + (2/3)a(T_1), \tag{18}$$

$$a(D_1) = (-1/3)a(R) + (4/3)a(T_1). \tag{19}$$

If we use high field high frequency EPR, these overlapped spectra will be separated and can be assigned easily. This was realized by a time-resolved W-band (95 GHz) EPR.[29–31] With this method not only the Q_1 and D_0 states appeared at the X band but also the D_1 state were assigned based on the observed g value (2.0016) and Eq. 15. This was the first observation of the D_1 signal in solution for a radical–triplet pair system.[30] The better spectra were obtained at both bands for ZnTPP–3Nopy, as shown in Fig. 15.[31] Here the decay curve was obtained at each field, as shown in Fig. 16, where the decay is different for the Q_1 and D_1 states. This result indicates that
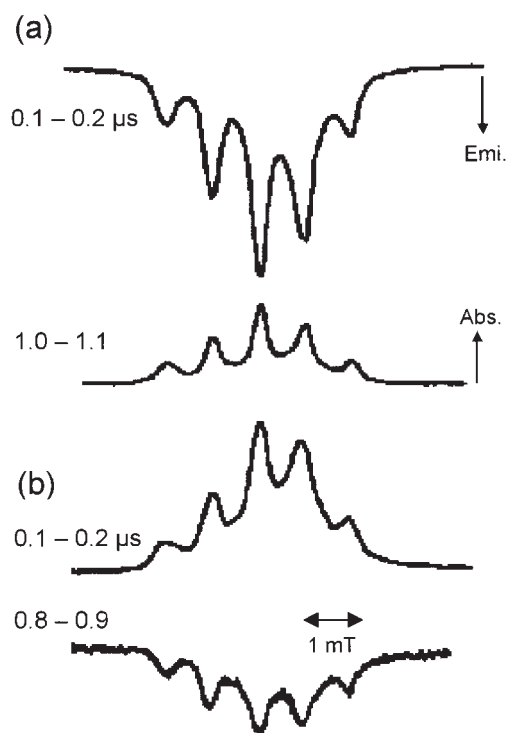

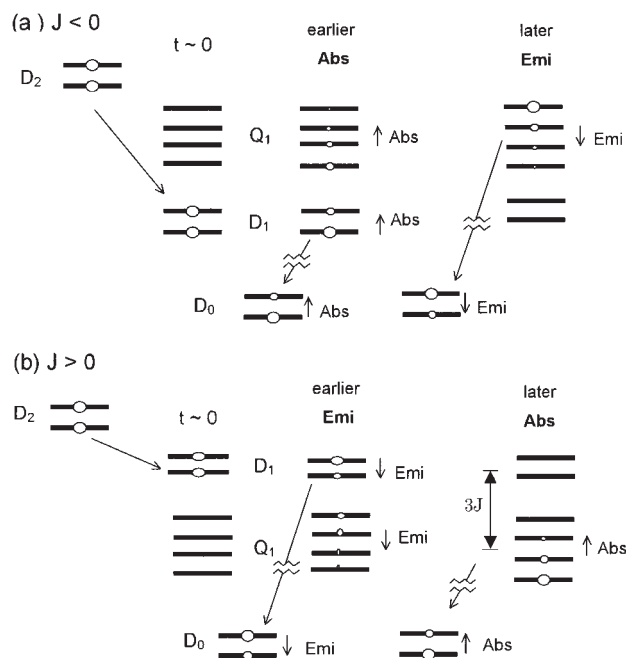Fig. 13. Time-resolved EPR spectra of a) MgTPP–4-Nitpy and MgTPP–3-Nitpy in toluene at room temperature.

Fig. 14. Schematic demonstration of relation between a sign of J and polarization inversion ($E \rightarrow A$ or $A \rightarrow E$) with time.

the populations of the Q_1 and D_1 states are not completely in equilibrium. It is very important to analyze these decay curves both at the X- and W-bands, which is now in progress. In order to simulate these decay curves, we first obtained the decay rate constants of the excited multiplet states by flash photolysis in several systems as summarized in Table 5. It is found that the
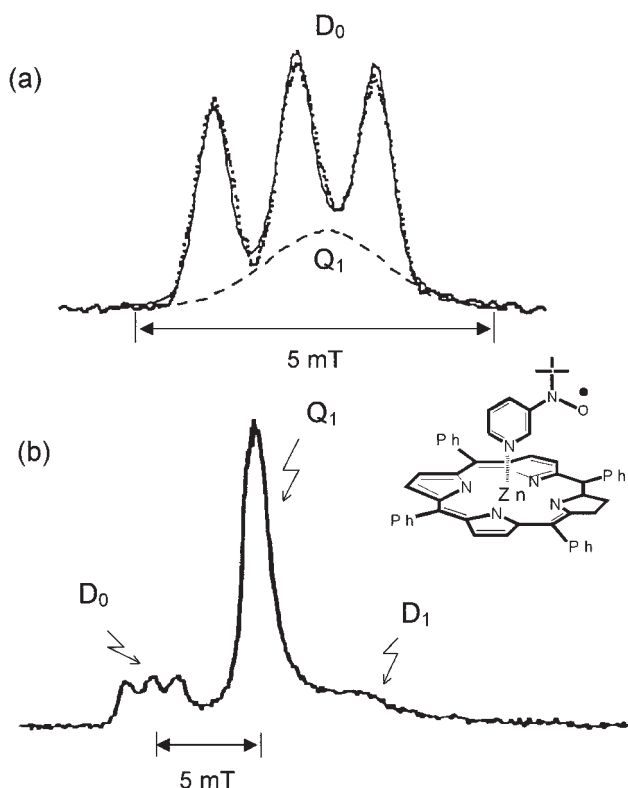
(a)

(b)

Fig. 15. a) X-band (9.5 GHz) and b) W-band (95 GHz) EPR spectra of ZnTPP–3-Nopy observed in toluene at room temperature and 0–50 ns and 100–200 ns after the laser pulse, respectively. The excited quartet (Q_1) and doublet (D_1) states signals are found together with the ground state (D_0) signal.

Table 5. Decay Rate Constant k_{D1}[a] of the Excited Doublet States in Different Systems

Systems	$k_{D1}/10^6$ s^{-1}
ZnTPP–3-Nopy	14
ZnPc–3-Nopy	0.86
ZnPc–4-Nopy	≥ 80

a) The value of k was obtained from the observed decay rate k_{obs} of the excited multiplet state and the equation of $k_{D1} = 3k_{obs}$ [Ref. 33].

decay rates are different by a factor of ca. 100 among the similar systems.

As for excited state dynamics, static EPR parameters such as the g value and the linewidth of the Q_1 state are useful to determine the exchange (ISC) rate between the Q_1 and D_1 states, when these two states are exchanged together. From the simulation of the spectra on the basis of numerical calculations using the modified Bloch equations, the ISC rate was estimated as 1.2×10^8 and 6×10^7 s^{-1} for the ZnTPP–3-Nopy complex at the X- and W-bands, respectively.[32]

Ishii et al. have reported extensive studies on the ZnPc–NRX and –RX (X = 1, 2; the number of the radicals) systems in fluid solution by means of TREPR, transient absorption, and fluorescence.[33] Correlations between spin polarization, an exchange interaction, and a lifetime of the excited multiplete state were
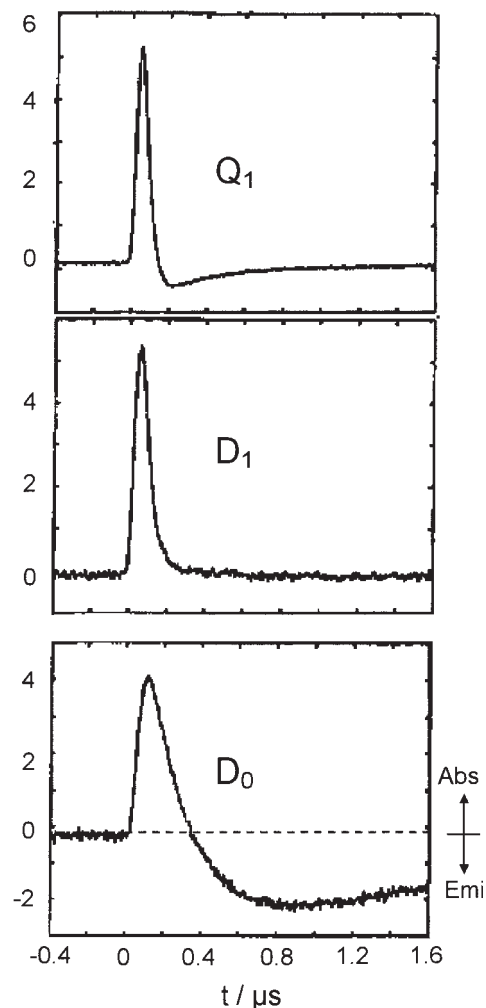

Fig. 16. W-band EPR decay curves for the Q_1, D_1, and D_0 states of ZnTPP–3-Nopy in toluene at room temperature obtained at the corresponding resonance fields (refer to Fig. 15b).

discussed. It was found that the electron spin polarization changes from the spin–orbit coupling type to the Q_1–D_1 mixing (RTPM) type, and that the lifetime becomes shorter from 15 (NR6) to 0.86 µs (NR4) and 7.6 (R1) to 3.7 (R2), with increasing the exchange interaction between T_1 and R. In the R2 system, they also found a novel spin polarization inversion ($E \rightarrow A$) in the triplet ground (T_0) state and interpreted it in terms of selective ISC (E) in the excited states and selective population to T_0 (A).

2. Fullerenes. In 1995 the Corvaja group reported a TREPR spectrum for nitroxide radical linked fullerene in fluid toluene solution and they assigned it to the Q_1 state using an isotropic hfcc and a g value.[8] They have developed such studies on different radical systems and those in solid state.[34] The polarization patterns and dynamic behaviors were analyzed and discussed in terms of spin polarization RTPM, the exchange interaction parameter J and decay kinetics. In solid state, we assigned the spectrum in a similar system to the quartet state and separated it into each spin component by means of two dimensional (2D) nutation spectroscopy.[35] Recently, both the excited quintet ($S = 2$) and triplet ($S = 1$) states were assigned in

S. Yamauchi

Bull. Chem. Soc. Jpn., **77**, No. 7 (2004)   1265

two nitroxides linked fullerene systems with the 2D nutation and TREPR techniques.

2.1 Studies by Corvaja Group: A first spectrum of the Q_1 state in fluid solution was observed for nitroxide radical linked fullerene (C_{60}) as shown in Fig. 17.[8] The spectrum is definitively assigned as that of the Q_1 state on the basis of the *g* value and hfcc with Eqs. 14 and 18. Although the obtained *g* value (2.0043) is a bit larger than the calculated one (2.0031), the hfcc (5.05 G) is just the same as the expected value ($a(D_0)/3 = 15.20/3 = 5.07$ G). The observed polarization E → A is interpreted by the RTPM of a triplet precursor (Fig. 14) as described in Sec. 1.2. A series of C_{60} derivatives containing an NO radical were examined in fluid solution as well as in solid matrix for both the ground and the excited quartet states. An opposite polarization pattern was found for molecules with different spacers between the triplet and the radical and is interpreted
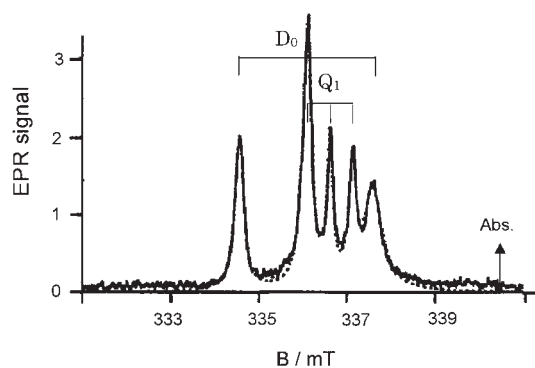

Fig. 17. First excited quartet (Q_1) spectrum observed in toluene solution by Corvaja et al. [Ref. 8]. D_0 denotes to the ground state signal.

by a different sign of *J* in the system. The time evolutions of the EPR signals were fitted by a kinetic model taking account the quartet decay rate, its branching ratio, and spin lattice relaxation rates,[31a] although these parameters are not confirmed yet. Photoinduced electron transfer from the quartet state was also analyzed by the time profiles of the Q_1 and D_0 signals.[31b] In all time-domain experiments, there seems to remain a problem that the time resolution of the TREPR apparatus is not fast enough to analyze completely the overall dynamics of the excited states.

2.2 1D and 2D EPR in Solid: In solid state, nitroxide linked fullerene provided a less structured TREPR spectrum in the excited state due to small ZFS and large inhomogeneous linewidths. It is very difficult to assign the observed spectrum, even its spin multiplicity, only from the one dimensional (1D) spectrum. In such a case, the 2D nutation technique is very powerful for the assignment of the state as described in the Experimental section. An example is shown in the following. The 1D spectrum was observed for two nitroxide radicals linked to fullerene, as shown in Fig. 18a at 20 K. The corresponding 2D spectrum was obtained as shown in Fig. 18b, where one axis is towards the magnetic field and the other indicates the nutation frequency.[32a] From the observed and calculated (Table 1) nutation frequencies, we can easily assign the spin multiplicity and magnetic transitions. The result shows an involvement of the doublet ground state (D_0) and the quintet states of $\pm 2 \leftrightarrow \pm 1$ (Q_u) and $\pm 1 \leftrightarrow 0$ (Q'_u) transitions. This was the first observation of an excited quintet state in the triplet–radical pair system. More importantly, when the 2D spectrum is sliced at an appropriate nutation frequency, the overlapped spectra are separated into each component of the spin state, as shown in Figs. 19a, 19b, and 19c. From the result, it is found for this bisradical ad-
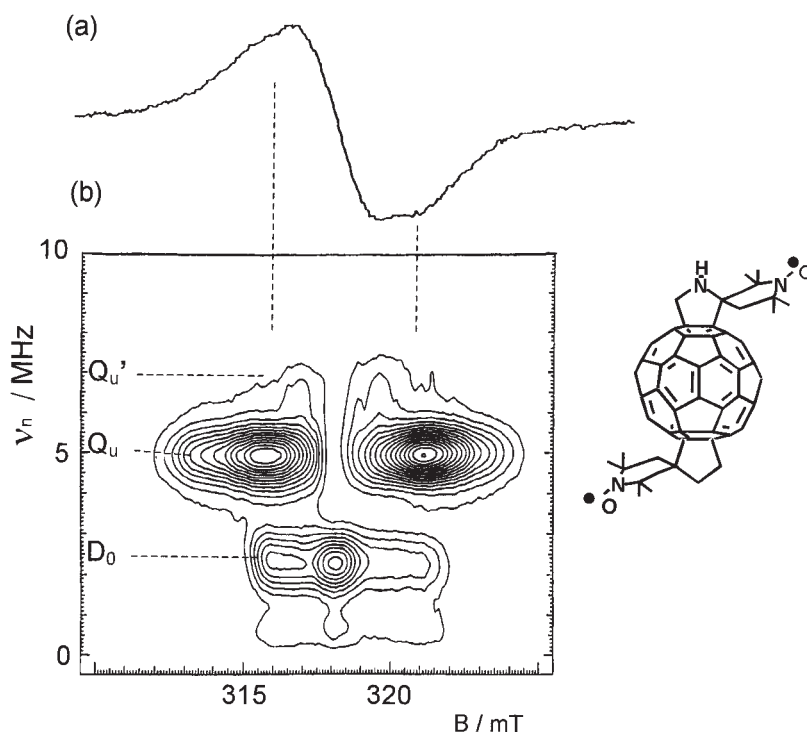

Fig. 18. a) One dimensional and b) two dimensional EPR spectra of two nitroxide radicals linked fullerene in toluene at 20 K. From the nutation frequency (ν_n) two transitions of quintet states (Q_u and Q'_u) are assigned together with the ground state (D_0) signal.
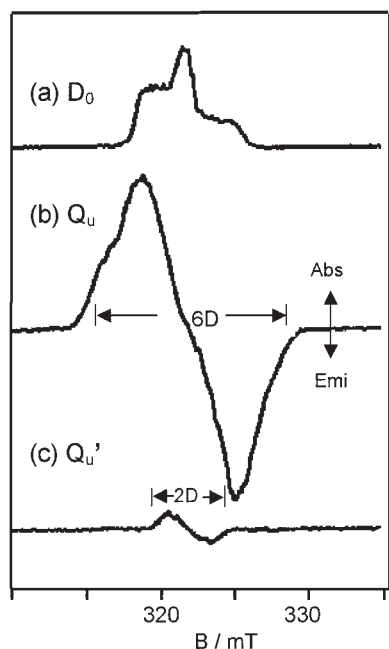
Fig. 19. Sliced spectra of the 2D spectrum (Fig. 18) for two nitroxide radicals linked fullerene, providing a pure ground state (D_0) spectrum and pure $|\pm1\rangle$–$|0\rangle$ (Q_u'), and $|\pm2\rangle$–$|\pm1\rangle$ (Q_u) transitions spectra in the quintet state.

duct that the T_1 ($S = 1$) and the radicals ($S = 1/2 \times 2$) couple ferro-magnetically generating the excited quintet state and that the two linked radicals couple very weakly and behave as a doublet state ($S = 1/2$) in the ground state. This indicates that photo-excitation induces couplings of two radicals via an excited triplet state, generating new magnetism. The consistent D value was obtained as $|D| = 60$ MHz from both the transitions, Q_u ($6D$) and Q_u' ($2D$), in the quintet state. In similar fullerene bis-radical adduct systems, the same analyses have been applied.[32b,33]

A 1D spectrum plays an important role in several cases: one is a case where the excited states decay fast and the nutation cannot be observed. Another is a case that spin–spin relaxation is too fast to observe the nutation. We have met this latter case in several bis-radical adducts of fullerene, where the excited states signals could be observed for the quintet but not for the triplet in the pulsed experiment.[36] In contrast, both the quintet and T_1 signals were observed in the 1D TREPR spectrum. Here the nutation was not observed for the triplet signals but was observed for the quintet ones, which is consistent with the 2D experiment. When we select the delay time when the quintet signal crosses the zero line due to nutation, only the triplet spectra were obtained as shown in Fig. 20. This is the first observation of the T_1 state in the strongly coupled triplet–biradical pair system.[36,37] The observed very fast spin–spin relaxation was interpreted by a very fast inter-conversion occurring between two close-lying triplet (T_1 and T_2) states. The 2D nutation technique is also not applicable to systems in solution where the whole excitation is achieved by pulsed microwave excitation. In this case, high field high frequency EPR is useful to assign the spin state as mentioned above (Sec. 1.2).

3. Other Systems. The studies on excited triplet–radical(s)/ unpaired electron(s) interactions are extended to other systems
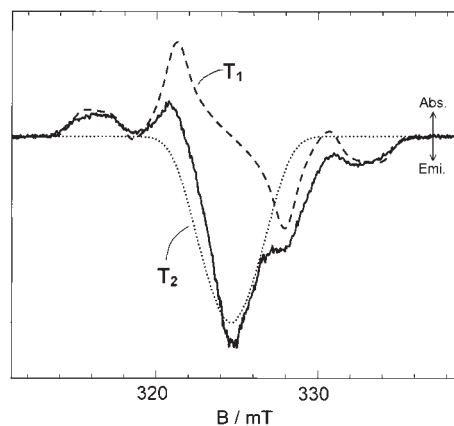

Fig. 20. Time-resolved EPR spectra of the two triplet states for two nitroxide radicals linked fullerene at 40 K; straight line: observed spectrum, dotted and broken lines: two excited triplet ones. The spectrum was observed at ca. 700 ns after the laser pulse where the quintet signals cross the base line and make almost no contribution.

such as porphyrin hybrid dimers and anthracene derivatives by the Asano group and the Teki group, respectively. In linked copper porphyrin (CuP; $S = 1/2$)–free base porphyrin (H_2P) dimers, Asano et al. found novel spin polarization for the energy acceptor part of H_2P, which cannot be analyzed by any ISC process.[38] They have analyzed this polarization in terms of a specific deactivation process of triplet H_2P due to a weak coupling between the triplet and an unpaired electron of the Cu atom. The fast deactivation and spin relaxations in the excited doublet D_1 state are considered to be involved in this process.[39]

Teki et al. extended the triplet–radical pair system to a π-conjugated system of dipenylanthracene (DPA)–iminonitroxide(s) and have observed spectra of both the excited quartet and quintet states.[40] In this case strong interactions are involved between the triplet and radical(s), providing a larger exchange coupling J among the excited multiplet states and a larger spin orbit coupling contribution from the radical NO part. These properties result in a unique relaxation and spin polarization in the multiplet states. They also examined a spin alignment effect on spin polarization using isomer radicals and have found that the interactions are ferromagnetic and anti-ferromagnetic depending on the position of the radical. Such results indicated the existence of a spin alignment and an important role of π-topology in their system.

Conclusion

We have extended time-resolved EPR (TREPR) spectroscopy to studies on the electronic excited states in fluid solution. TREPR spectra reflecting zero field splitting (ZFS) parameters were observed for the first time by use of tetraphenylporphyrins (MTPP: M = Zn, Mg, and H_2) in the excited triplet (T_1) states. For phthalocyanines and subphthalocyanine, T_1 spectra were also observed in solution. Temperature dependences of the spectra have been analyzed by simulations on the basis of a discrete jump model among N ($N = 1, 2, 3, \ldots$) sites with different exchange rates at 5–360 K in toluene. It is found that several excited states and molecular rotations are involved in the temperature dependent spectra. For example, the two Jahn–Teller

S. Yamauchi

Bull. Chem. Soc. Jpn., **77**, No. 7 (2004)   1267

split states and two kinds of excited (a_{1u}–e_g and a_{2u}–e_g) triplet states were observed in metalloporphyrins (ZnTPP and MgTPP). The molecular rotations were also observed for all molecules examined and usually changed from in-plane to out-of-plane motions. For all processes, the activation energy or energy difference is obtained from the temperature dependence of the exchange rates. These results indicate that photochemical reactions could be controlled (selected) in an appropriate temperature range.

A new type of excited spin (excited multiplet) states was generated by use of T_1–radical pairs and observed by EPR spectroscopy. More importantly the spin states were assigned and characterized by various kinds of advanced EPR techniques. High field high frequency EPR is useful for observations of the multiplet states in fluid solution and two-dimensional pulsed EPR is useful for those in solid solution. Various excited multiplet states such as doublet ($S = 1/2$), triplet ($S = 1$), quartet ($S = 3/2$), and quintet ($S = 2$) states were assigned and characterized in this system. The ZFS parameters, hyperfine coupling constants, and linewidths were analyzed in terms of electronic structures and dynamics in the excited states. Especially, the lifetime of the excited multiplet state has been found to be very sensitive to the electronic structures of the T_1 and radicals. This result could shed light on control of the lifetime in the excited state and/or intermediate species in photochemical reactions.

References

1   a) N. Hirota and S. Yamauchi, "Dynamics of Excited Molecules," ed by K. Kuchitsu, Elsevier, Amsterdam (1994), pp. 513–557. b) N. Hirota and S. Yamauchi, "Dynamic Spin Chemistry," ed by S. Nagakura, H. Hayashi, and T. Azumi, Kodansha, Tokyo (1998), pp. 187–247.

2   N. Hirota and S. Yamauchi, *J. Photochem. Photobiol., C*, **4**, 109 (2003).

3   C. A. Hutchison and B. W. Mangum, *J. Phys. Chem.*, **29**, 952 (1958).

4   a) G. L. Closs, P. Gautam, D. Zhang, P. Crusic, S. A. Hill, and E. Wasserman, *J. Phys. Chem.*, **96**, 5528 (1992). b) A. Regev, D. Gamliel, V. Meiklyer, S. Michaeli, and H. Levanon, *J. Phys. Chem.*, **97**, 3671 (1993).

5   J. Fujisawa, Y. Ohba, and S. Yamauchi, *J. Am. Chem. Soc.*, **119**, 8736 (1997).

6   H. Levanon, *Rev. Chem. Intermed.*, **8**, 287 (1987).

7   G. Kothe, S. S. Kim, and S. I. Weissman, *Chem. Phys. Lett.*, **71**, 445 (1980).

8   C. Corvaja, M. Maggini, M. Prato, G. Scorrano, and M. Venzin, *J. Am. Chem. Soc.*, **117**, 8858 (1995).

9   K. Ishii, J. Fujisawa, Y. Ohba, and S. Yamauchi, *J. Am. Chem. Soc.*, **118**, 13079 (1996).

10   S. Ohkoshi, S. Yamauchi, Y. Ohba, and M. Iwaizumi, *Chem. Phys. Lett.*, **224**, 313 (1994).

11   a) T. F. Rrisner, M. Rohrer, and K. Möbius, *Appl. Magn. Reson.*, **7**, 167 (1994). b) O. Burghaus, M. Rohrer, T. Götzinger, and K. Möbius, *Meas. Sci. Technol.*, **3**, 75 (1992).

12   a) R. Hanaishi, Y. Ohba, S. Yamauchi, and M. Iwaizumi, *J. Chem. Phys.*, **103**, 4819 (1995). b) R. Hanaishi, Y. Ohba, S. Yamauchi, and M. Iwaizumi, *Bull. Chem. Soc. Jpn.*, **69**, 1533 (1996).

13   a) N. Mizuochi, Y. Ohba, and S. Yamauchi, *J. Phys. Chem. A*, **101**, 5966 (1997). b) N. Mizuochi, Y. Ohba, and S. Yamauchi, *J. Chem. Phys.*, **111**, 5966 (1999).

14   a) A. Abragam, "The Principles of Nuclear Magnetism," Clarendon Press, Oxford (1961). b) G. Kroll, M. Plüschau, K.-P. Dinse, and H. van Willigen, *J. Chem. Phys.*, **93**, 8709 (1990).

15   a) M. R. Wasielewski, M. P. O'Neil, K. R. Lykke, M. J. Pellin, and D. M. Gruen, *J. Am. Chem. Soc.*, **113**, 2774 (1991). b) P. A. Lane, L. S. Swanson, O.-X. Ni, J. Shinar, J. Engel, T. J. Barton, and L. Jones, *Phys. Rev. Lett.*, **68**, 887 (1991).

16   C. A. Stern, H. van Willigen, and K.-P. Dinse, *J. Phys. Chem.*, **98**, 7464 (1994).

17   a) J. Fujisawa, K. Ishii, Y. Ohba, M. Iwaizumi, and S. Yamauchi, *J. Phys. Chem.*, **99**, 17082 (1995). b) J. Fujisawa, K. Ishii, Y. Ohba, M. Iwaizumi, and S. Yamauchi, *J. Phys. Chem. A*, **101**, 434 (1997).

18   S. Yamauchi, A. Takahashi, Y. Iwasaki, M. Unno, Y. Ohba, J. Higuchi, A. Blank, and H. Levanon, *J. Phys. Chem. A*, **107**, 1478 (2003).

19   S. Yamauchi, H. Ogasawara, Y. Iwasaki, J. Fujisawa, Y. Ohba, B. Aharon, and H. Levanon, unpublished results.

20   S. I. Weissman, *J. Phys. Chem.*, **29**, 1189 (1958).

21   I. SM Saiful, J. Fujisawa, N. Kobayashi, Y. Ohba, and S. Yamauchi, *Bull. Chem. Soc. Jpn.*, **72**, 661 (1999).

22   O. Gonen and H. Levanon, *J. Phys. Chem.*, **84**, 4132 (1986).

23   J. R. Norris and S. I. Weissman, *J. Phys. Chem.*, **73**, 3119 (1969).

24   A. Hudson and A. D. McLachlan, *J. Phys. Chem.*, **43**, 1518 (1965).

25   a) K. Ishii, S. Yamauchi, Y. Ohba, and M. Iwaizumi, The 33rd Japan ESR Symposium, Sendai, Japan (1994), p. 103. b) K. Ishii, S. Yamauchi, Y. Ohba, and M. Iwaizumi, The 53rd Okazaki Conference, Okazaki, Japan (1995), p. 16.

26   A. Bencini and D. G. Gatteschi, "EPR of Exchange Coupled Systems," Springer-Verlag, Berlin (1990), pp. 49–57.

27   K. Ishii, J. Fujisawa, A. Adachi, S. Yamauchi, and N. Kobayashi, *J. Am. Chem. Soc.*, **120**, 3152 (1998).

28   a) K. Ishii, T. Ishizaki, and N. Kobayashi, *J. Phys. Chem. A*, **103**, 6060 (1999). b) K. Ishii, T. Ishizaki, and N. Kobayashi, *Appl. Magn. Reson.*, **23**, 369 (2003).

29   J. Fujisawa, K. Ishii, Y. Ohba, S. Yamauchi, M. Fuhs, and K. Möbius, *J. Phys. Chem. A*, **101**, 5869 (1997).

30   J. Fujisawa, K. Ishii, Y. Ohba, S. Yamauchi, M. Fuhs, and K. Möbius, *J. Phys. Chem. A*, **103**, 213 (1999).

31   J. Fujisawa, Y. Iwasaki, Y. Ohba, S. Yamauchi, N. Koga, S. Karasawa, M. Fuhs, K. Möbius, and S. Weber, *Appl. Magn. Reson.*, **21**, 483 (2001).

32   Y. Iwasaki, K. Katano, Y. Ohba, S. Karasawa, N. Koga, and S. Yamauchi, *Appl. Magn. Reson.*, **23**, 377 (2003).

33   a) K. Ishii, S. Takeuchi, and N. Kobayashi, *J. Phys. Chem. A*, **105**, 6794 (2001). b) K. Ishii, T. Ishizaki, and N. Kobayashi, *J.*

Am. Chem. Soc., **123**, 702 (2001).

34   a) C. Corvaja, M. Maggini, M. Ruzzi, G. Scorrano, and A. Troffoletti, *Appl. Magn. Reson.*, **12**, 477 (1997). b) F. Conti, C. Corvaja, M. Maggini, P. Piu, G. Scorrano, and A. Troffoletti, *Appl. Magn. Reson.*, **13**, 337 (1997).

35   a) N. Mizuochi, Y. Ohba, and S. Yamauchi, *J. Phys. Chem. A*, **103**, 7749 (1999). b) F. Conti, C. Covaja, A. Toffoletti, N. Mizuochi, Y. Ohba, and S. Yamauchi, *J. Phys. Chem. A*, **104**, 4962 (2000).

36   Y. Ohba, M. Nishimura, N. Mizuochi, and S. Yamauchi, *Appl. Magn. Reson.*, in press.

37   For a weakly coupled system, refer to C. Corvaja, L.

Franco, and M. Mazzoni, *Appl. Magn. Reson.*, **20**, 71 (2001).

38   M. Asano-Someda, T. Ichino, and Y. Kaizu, *J. Phys. Chem.*, **101**, 3479 (1997).

39   a) M. Asano-Someda, A. van der Est, U. Krüger, D. Stehlik, Y. Kaizu, and H. Levanon, *J. Phys. Chem. A*, **103**, 6704 (1999). b) A. van der Est, M. Asano-Someda, P. Ragogna, and Y. Kaizu, *J. Phys. Chem. A*, **106**, 8531 (2002).

40   a) Y. Teki, S. Miyamoto, K. Iimura, M. Nakatsuji, and Y. Miura, *J. Am. Chem. Soc.*, **122**, 984 (2000). b) Y. Teki, S. Miyamoto, M. Nakatsuji, and Y. Miura, *J. Am. Chem. Soc.*, **123**, 294 (2001).

Seigo Yamauchi was born in 1948 in Aizuwakamatsu, Japan. He did his Ph. D. studies at Tohoku University with Professor Tohru Azumi on "Triplet Sublevel Properties of Aromatic Molecules by Zero-field ODMR" and obtained the degree in 1976. He spent two years at the University of Pittsburgh as a postdoctoral fellow in Professor David W. Pratt's laboratory and started ODESR experiments. In 1979 he joined the Chemistry Department at Kyoto University, working with Professor Noboru Hirota on time-resolved EPR studies in the photochemistry of organic molecules. In 1989, he moved to Sendai and is currently a Professor of Chemistry in the Institute of Multidisciplinary Research for Advanced Materials (IMRAM) at Tohoku University. His research interests are in the photo-physics and photochemistry of composite molecules, including metal complexes and biomolecules, by means of time-resolved and pulsed EPR and resonance Raman spectroscopy.